Finite element and automatic remeshing methods for the simulation of complex blow molded polymer components

Michel Bellet, Andres Rodriguez-Villa*, Jean-François Agassant

Ecole des Mines de Paris, CEMEF, Centre de Mise en Forme des Matériaux, URA CNRS 1374, BP207, F-06904 Sophia Antipolis, France

**Transvalor S.A., Les Espaces Delta, BP 37, F-06901 Sophia Antipolis Cedex, France*

in: Simulation of Materials Processing: Theory, Methods and Applications Proc. NUMIFORM'98, 6th Int. Conf. on Numerical Methods in Industrial Forming Processes, Enschede, The Netherlands, 22-25 June 1998, J. Huétink, F.P.T. Baaijens (eds.), Balkema, Rotterdam, pp. 489-494 (1998)

ABSTRACT: This paper presents a three dimensional finite element model of the extrusion blow molding process. The code Tform3 has the following characteristics: membrane formulation, linear triangle elements, updated Lagrangian implicit formulation, viscoelastic differential constitutive equations. The paper presents a brief recall of the formulation and then addresses three key issues of the simulation: automatic identification of constitutive equation parameters, automatic remeshing, coupling between gas pressure and inflation. An example of application to the extrusion blow molding of a bottle is presented.

1 INTRODUCTION

The extrusion blow-molding process consists in blowing an extruded cylindrical thin tube, or parison, of molten polymeric material (polyethylene, polyester, polyvinylchloride) into a mold. The process is applied to the production of hollow components such as bottles and tanks.

One of the key problems in product development is the fulfilment of a prescribed thickness distribution of the final part. Obviously numerical simulation can help in process optimisation and the finite element software Tform3 has been developed in that sense. After a brief recall of its basic concepts, the paper will focus on three key issues: automatic identification of rheology parameters, automatic remeshing, and coupling between internal gas pressure and inflation kinetics.

2 TFORM3. FEM MEMBRANE MODEL

Due to the reduced thickness of inflated parisons with respect to their curvature radii, it is possible to consider them in a first approach as geometrical surfaces, or membranes. This is equivalent to neglecting the mechanical power dissipated by flexion and shear through thickness with respect to the power of tangential expansion. In other words, the stress state is considered planar in the tangent plane to each point of the membrane.

Membrane assumption is done by most of the authors for polymer blowing finite element analysis (thermoforming or extrusion blow-molding process). Let us quote Warby & Whiteman 1988, Charrier et al. 1989, De Lorenzi & Nied 1991, Kouba et al. 1992, Shrivastava & Tang 1993, Vantal et al. 1995, Rodriguez-Villa et al. 1995, Santhanam et al. 1995, Zhang et al. 1995, Laroche et al. 1996. It should be noted that some authors, in this context, use an explicit formulation based on a centered finite differences scheme (equivalent to a resolution for the acceleration variable) (Rachik et al. 1994, D'Oria et al. 1995, Verron 1997), whereas others prefer an implicit formulation, using the velocity or displacement as primitive variable. As the inertia terms are generally weak or moderate in extrusion blow-molding processes, the software Tform3 has been based on an implicit scheme.

The alternatives to the membrane assumption are on one hand the shell formulation, not frequently used in this field, probably because of its low increase of precision as compared to the membrane one, and, on another hand, the volumic formulation. Let us quote Song et al. 1991 for thermoforming, Debbaut et al. 1993, Hartwig & Michaeli 1995, Schmidt et al. 1996 for blow-molding. These authors stress the point that this formulation is interesting in presence of significative shear through the thickness, due to the tooling (stretching rod, punch). Another reason is the heat transfer analysis, although this can be accounted for in membrane formulation (Vantal et al. 1995).

In our formulation, we define a system of two curvilinear coordinates onto the inflated membrane. The mechanical equilibrium is expressed by the principle of virtual power according to the following equation (Bellet et al. 1990):

$$\forall \mathbf{v}^* \int_\Omega \sigma^{ij} v^*_{i|j} \, e dS - \int_{\Omega_p} p_d \mathbf{g}_3 . \mathbf{v}^* dS = 0 \qquad (1)$$

in which e is the local thickness, p_d is the differential pressure applied to the region Ω_p of the deformed parison Ω, $\boldsymbol{\sigma}$ is the Cauchy stress tensor of contravariant components σ^{ij}, $\mathbf{g}_3$ is the normal vector to the membrane, $\mathbf{v}^*$ is any virtual velocity field of covariant derivative components $v^*_{i|j}$. According to the membrane assumption, i,j=1,2.

In this equation, gravity and friction effects have been neglected. Hence a sticking contact is

considered, which is representative of actual contact between hot polymer and cold metallic tools.

At each time increment $[t,t+\Delta t]$, given an initial balanced configuration Ω^t, the problem consists in solving (1) at time $t+\Delta t$. An implicit time integration scheme for the velocity is used and therefore, using the constitutive and incompressibility equations, (1) can be solved for the single unknown velocity field $\mathbf{v}^{t+\Delta t}$.

Discretisation with linear triangles yields a set of non-linear equations which is solved by the Newton-Raphson method. Then the configuration is updated.

A contact algorithm computes the position of each node with respect to the tooling surfaces, which are discretised with triangles. When a node penetration has been detected, the algorithm computes the normal velocity to be prescribed during next time increment in order to bring the node back onto the tool surface. According to the sticking contact assumption, the relative velocity of contacting nodes with respect to the tool is prescribed to zero.

3 CONSTITUTIVE EQUATION AND IDENTIFICATION

The pioneer works on blow-molding use hyperelastic constitutive equations, invoking short forming times. The most frequent models are Mooney-Rivlin and Ogden ones: Charrier et al. 1989, De Lorenzi & Nied 1991. This approach is still popular: Rachik et al. 1994, Hartwig & Michaeli 1995, D'Oria et al. 1995, Santhanam et al. 1995, Laroche et al. 1996.

However, molten polymer rheology is viscoelastic, and most authors naturally use an extension of hyperelastic laws, i.e. integral viscoelastic models. The pioneer work of Warby & Whiteman 1988 in this field has been followed by Kouba et al. 1992 with K-BKZ model, Shrivastava & Tang 1993, Verron 1997 with Christensen model. Others prefer differential viscoelastic models: Debbaut et al. 1993 with Giesekus law, Rachik et al. 1994 with White-Metzner model, Schmidt et al. 1996 and Rodriguez-Villa et al. 1995, 1997 with Maxwell, Oldroyd-B and Phan-Tien & Tanner models. Those last three constitutive equations are implemented in Tform3.

3.1 *Maxwell viscoelastic model*

The upper-convected Maxwell model is expressed by:

$$\boldsymbol{\sigma} = -p\mathbf{I} + \mathbf{T}_v \tag{2}$$

$$\mathbf{T}_v + \lambda \frac{\delta \mathbf{T}_v}{\delta t} = 2\mu\dot{\boldsymbol{\varepsilon}} \tag{3}$$

where p is an arbitrary pressure, $\mathbf{T}_v$ the extra-stress tensor, λ the relaxation time, μ the dynamic viscosity and $\delta\mathbf{T}_v/\delta t$ the upper-convected Oldroyd's derivative:

$$\frac{\delta \mathbf{T}_v}{\delta t} = \frac{d\mathbf{T}_v}{dt} - [\mathbf{Grad\ v}]\,\mathbf{T}_v - \mathbf{T}_v[\mathbf{Grad\ v}]^T \tag{4}$$

It is to be noticed that this upper-convected derivative reduces in curvilinear coordinates to the total derivative of covariant components (Bellet et al. 1990, Rodriguez-Villa et al. 1995).

3.2 *Identification by inverse method*

This method consists in the association of an instrumented blow molding test with a procedure of automatic identification using the finite element simulation of the test (Rodriguez-Villa 1997).

The mold shape is shown at figure 1. The inflation is recorded through a lateral window, using a video recorder at 25 pictures.s^{-1} (the typical inflation time being in the range 0.6 to 3 s.).

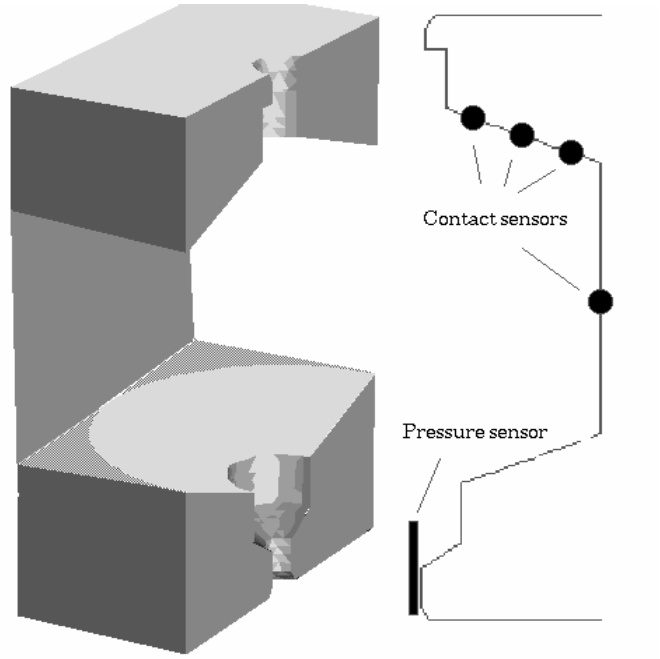

Figure 1. Instrumented mold.

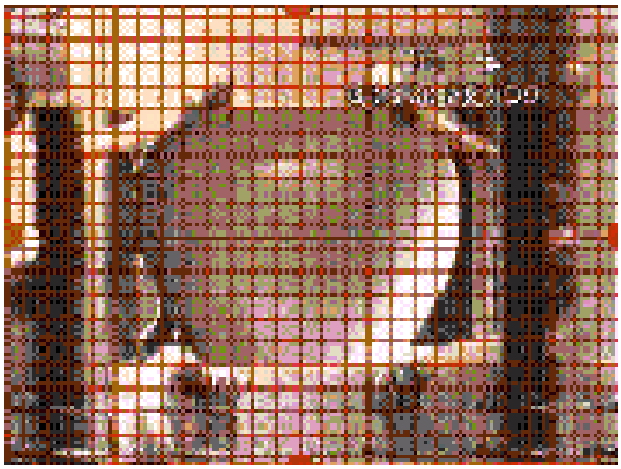

Figure 2. Video acquisition during inflation.

A recording example is given at figure 2. It provides the measurement of the radius at mid-height of the parison as a function of time $R(t)$. In addition, the internal air pressure $p_a(t)$ is recorded (fig.3).

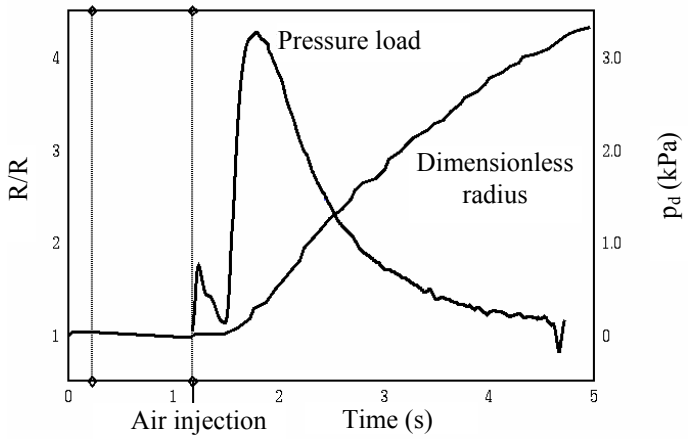

Figure 3. Measured differential air pressure: $p_d(t) = p_a(t) - p_{atm}$ (p_{atm} being the atmospheric pressure) and scaled parison radius vs time.

The reproducibility of such measurements has been checked for different inflation rates and temperatures. The identification step has been carried out as follows. Each blow molding test is simulated using the finite element software Tform3, applying to the parison the pressure load which has been effectively measured during the test. Then, by successive iterations, the set of parameters P (=(λ,μ) for Maxwell law) is modified until the error between the measured and the computed curves R(t) is reduced to a minimum. This error is defined as:

$$E(P) = \sum_{i=1}^{nexp} \left(R_i^{cal}(P) - R_i^{exp} \right)^2 \Big/ \sum_{i=1}^{nexp} \left(R_i^{exp} \right)^2 \qquad (5)$$

in which nexp is the number of sampling points. The minimisation of E is achieved by a Gauss-Newton method, needing the first derivatives of E, and therefore the derivatives of R_i^{cal} with respect to each parameter of P. Because of the very low computation time of the direct FEM simulation of the test, those derivatives are approached by finite differences.

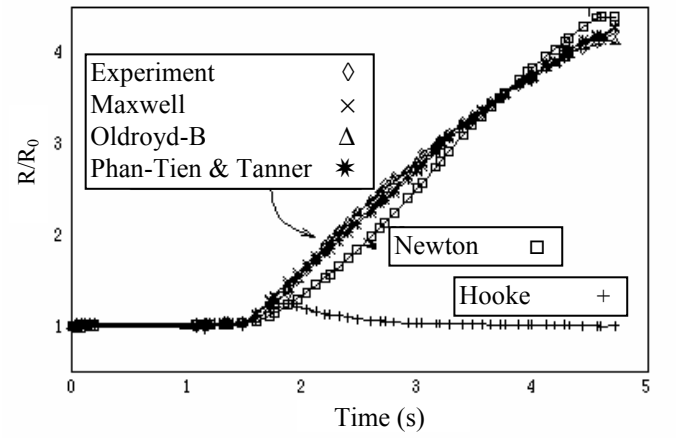

Figure 4. Automatic identification of the parameters of several constitutive equations on a blow molding test.

Figure 4 shows the comparison, for a single test, between experimental and computed (after optimization) curves R(t). It is found, as expected, that neither the linear elastic nor the Newtonian laws are able to account for the actual radius evolution under the measured pressure load. This clearly demonstrates the viscoelastic character of molten polymer during blow molding. For the three viscoelastic laws which have been tested (Maxwell, Oldroyd-B, Phan-Tien & Tanner), it has always been possible to exhibit a set of parameters resulting in a low error E. Table 1 gives the parameter values identified for a Maxwell constitutive equation on four blow molding tests for different inflation rates and temperatures. The dependence of viscosity on strain rate is shown in figure 5, with reference to measurements issued from shear and tensile tests.

T (°C)	$\dot{\varepsilon}_{eq}$ (s^{-1})	μ (Pa.s)	λ (s)	E (%)
180	0.4	54500	0.33	3.8
180	2.0	26800	0.035	6.8
200	1.05	35300	0.15	4.8
200	2.65	25500	0.05	7.4

Table 1. Maxwell viscosity and relaxation time identified by inverse method on four different blowing tests.

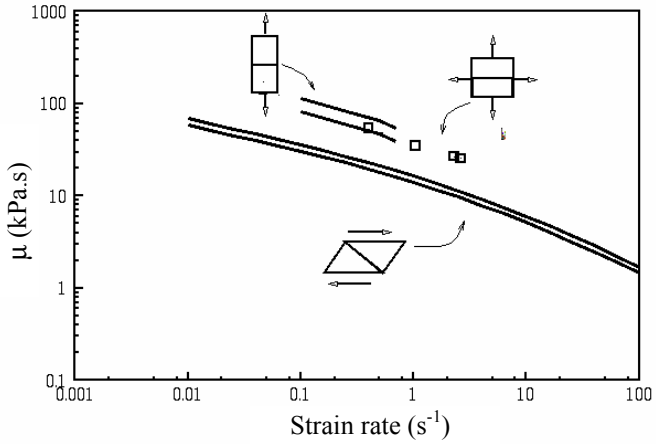

Figure 5. Comparison of viscosities measured in shear test, uniaxial tensile test and in the present blowing test.

The viscosity is found higher in blowing conditions (biaxial stretching) than in shear conditions and comparable to the elongational viscosity found in uniaxial tensile conditions at similar strain levels. The dependence of λ and μ on strain rate is similar to the one found in shear conditions. It can be concluded that the Maxwell law is representative - at least qualitatively - of actual phenomena. However, a much better quantitative agreement should be obtained on the whole set of tests using a generalized Maxwell model.

4 AUTOMATIC AND ADAPTIVE REMESHING

During blow molding, the material encounters large deformations. Hence the use of a simple updated Lagrangian formulation, consisting in convecting the mesh with the material, would result in a loss of precision due to mesh coarsening or mesh distortion.

This can be avoided by regenerating the mesh from time to time.

The problem consists in remeshing a warped triangulated surface. The algorithm is initially issued from the remeshing procedure of Forge3 software (Coupez 1996). The basic principle is to extract around each node or each mesh edge a sub-topology composed of the elements including the considered node or edge, as explained on figure 6. Alternative topologies are then built and evaluated using a quality criterion (see hereunder). The best topology is then fixed and reinserted in place of the initial one and another node or edge is examined. The procedure is stopped when no more topological changes are found necessary.

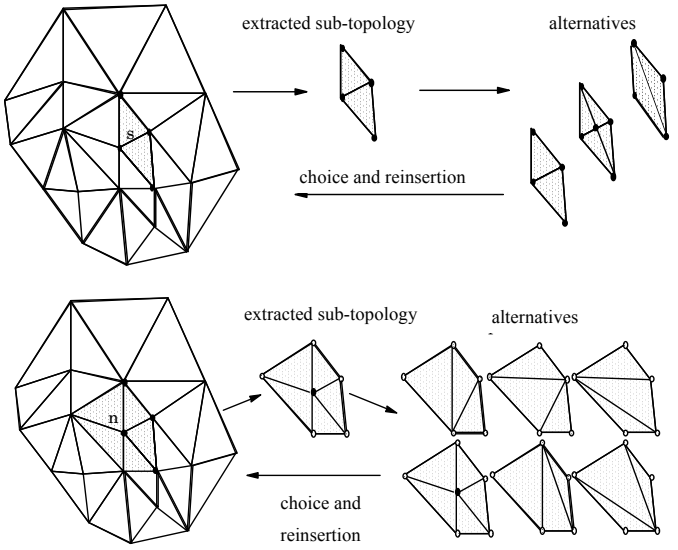

Figure 6. Extraction of sub-topology around an edge or a node. Choice among alternative sub-topologies and reinsertion.

The quality Q^τ of a sub-topology τ is taken equal to the minimum quality of its elements e:

$$Q^\tau = \underset{e\in\tau}{\text{Min}}\, Q^e \tag{6}$$

where Q^e denotes element quality, which takes into account both shape ratio and size.

The shape quality is defined by the ratio:

$$Q^e_{sh} = f S^e \Big/ \left(P^e\right)^2 \tag{7}$$

where S^e is the element surface, P^e its perimeter and f a coefficient such that the shape quality of equilateral triangles is equal to 1.

The size quality is defined by considering the deformation between the equilateral triangle of aimed size h_{obj} and the actual element (fig. 7).

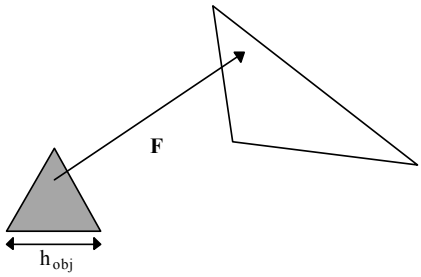

Figure 7. Transformation between aimed and actual element.

Denoting **C** the Cauchy dilatation tensor of transformation **F**, i.e. $\mathbf{C} = \mathbf{F}^T\mathbf{F}$, the size quality is defined by the formula:

$$Q^e_{sz} = \left(1 + Q^e_{sh}\left|\ln \mathbf{C}:\mathbf{C}\right|\right)^{-1} \tag{8}$$

in which it can be seen that the quality tends to 1 as **C:C** tends to 1 (which results in fact in producing elements smaller than the expected size h_{obj}). In addition, Q^e_{sz} is all the more discriminant as Q^e_{sh} is high. Finally, the element quality is determined by the product:

$$Q^e = Q^e_{sh}Q^e_{sz} = \frac{f S^e}{\left(P^e\right)^2\left(1 + Q^e_{sh}\left|\ln \mathbf{C}:\mathbf{C}\right|\right)} \tag{9}$$

Let us define now the aimed size h_{obj}. It results from an estimator of the geometric error associated with the current discretisation of the membrane. Such a problem has been addressed by Bonet (1994) and the present approach is similar. It is based first on a nodal smoothing of the tangent basis:

$$\tilde{\mathbf{g}}^n_i = \frac{1}{\sum_e S^e}\sum_e S^e \mathbf{g}^e_i \qquad i = 1, 2 \tag{10}$$

where the sum is extended to the elements e surrounding the considered node n. Then the deformation between the current and the smoothed surface can be measured by the Green-Lagrange type tensor:

$$L_{ij} = \frac{1}{2}\left(\tilde{g}_{ij} - g_{ij}\right) \tag{11}$$

This permits to define the local error as:

$$E^e = \frac{1}{S^e}\int_{\Omega^e} \mathbf{L}:\mathbf{L}\, dS \tag{12}$$

It can be shown that this error varies quadratically with element size h in the case of a regular cylindrical surface (Rodriguez-Villa 1997). Generalizing the same dependency, the aimed size h_{obj} can be defined by:

$$h_{obj} = h\sqrt{\frac{E_{obj}}{E}} \tag{13}$$

where E_{obj} and E are the objective error and the current local error respectively.

Finally, modifications of local topology are controlled by examining their impact on mean curvature variations.

5 PRESSURE / DEFORMATION COUPLING

Air pressure inside the parison has been recorded as a function of time during identification tests (fig. 3). It can be noticed that the measured pressure is considerably lower (by a ratio ranging from 30 to 100) than the nominal one in the upstream air feeding system. Moreover, the pressure is far from being constant during the inflation stage. The main pressure peak corresponds to the beginning of parison inflation: the radius significantly increases and at the same time the pressure decreases. This clearly demonstrates the coupling between inflation kinetics and pressure evolution.

In order to account for this phenomenon, a thermodynamic model has been developed (Rodriguez-Villa 1997). The specific air flow rate q_e (mass per time unit) is assumed constant, the air being in a given thermodynamic state (pressure p_e, specific mass ρ_e and temperature T_e). The energy variation of the air located inside the parison results from the energy input due to incoming air, from the energy dissipated by external forces and from the heat exchanged with the surroundings. This energy change is split into variations of internal energy, kinetic energy and potential energy:

$$dE = dE_e + \delta W + \delta Q = dU + dK + g\,dz \qquad (14)$$

Neglecting kinetic and potential energy variations, and assuming transformation adiabaticity, (14) can be written, expressing the work of external forces:

$$dE = dE_e - (p_a - p_{atm})\,dV = dU \qquad (15)$$

The specific energy of incoming air is denoted e_e, its internal energy u_e and its velocity v_e.

$$dE_e = \left(u_e + \frac{p_e}{\rho_e} + \frac{1}{2}v_e^{\,2}\right)dm = e_e q_e dt \qquad (16)$$

Combining (15) and (16) and using the relation $du = c_v dT$, in which c_v is the specific heat at constant volume, we have:

$$e_e q_e dt - (p_a - p_{atm})\,dV = m c_v dT + c_v T dm \qquad (17)$$

The air is then considered as a perfect gas, of constitutive equation $p_a V = m c_v (\gamma - 1) T$, with $\gamma = c_p / c_v$ the ratio of specific heats. The equation yielding the air pressure evolution p_a is then easily obtained:

$$\gamma p_a \frac{dV}{dt} - (\gamma - 1) p_{atm} \frac{dV}{dt} + V \frac{dp_a}{dt} = (\gamma - 1) e_e q_e \qquad (18)$$

Assuming that the blowing power $e_e q_e$ remains constant, it is then possible to determine it by a simple test of air blowing in a reservoir of constant volume V_c. In this case, $dV = 0$ and we have:

$$V_c \frac{dp_a}{dt} = (\gamma - 1) e_e q_e \qquad (19)$$

The blowing power can be estimated by measuring the initial pressure rate dp_a/dt, denoted $\dot{P}_0$. This parameter is a characteristic of the blowing machine. The pressure evolution during an extrusion blow molding on the same machine will be given by:

$$\gamma p_a \frac{dV}{dt} - (\gamma - 1) p_{atm} \frac{dV}{dt} + V \frac{dp_a}{dt} = V_c \dot{P}_0 \qquad (20)$$

A validation of this model has been carried out by coupling it to the computation of inflation kinetics in Tform3. Figure 8 gives an example – for one of the previous identification tests - of the good agreement between the measured pressure and the predicted one by the coupled model. From this result, it can be concluded that this coupling is definitely necessary to simulate extrusion blow molding in a realistic manner.

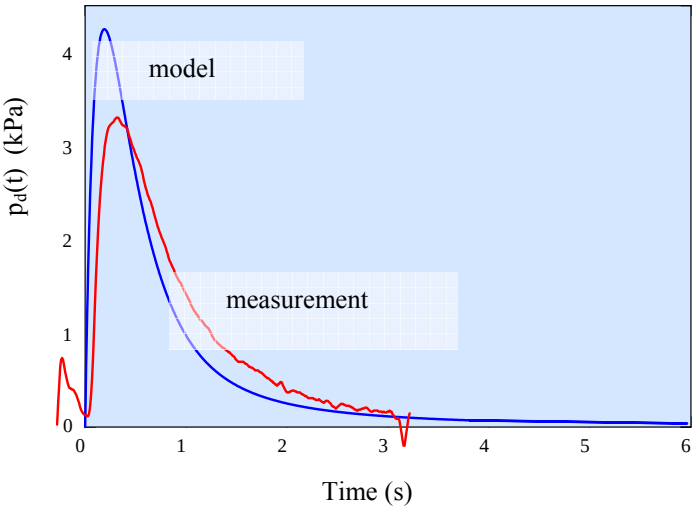

Figure 8. Comparison of measured and predicted pressure.

6 APPLICATION

Figure 9 shows a simulation of the extrusion blow molding of a detergent bottle made of high density polyethylene. The part encounters severe thickness gradients around its hollow handle. The initial geometry of the parison is: radius 60 mm, height 500 mm, thickness 1.5 mm. Due to the vertical symmetry, only half of the parison is computed. It is assumed to be fixed at the upper end (output of extrusion die) and a zero vertical displacement is prescribed at the lower end.

On this figure, the progressive onset of contact with the mold can be seen, during the closure of the mold, before the blowing itself. The efficiency of adaptive remeshing procedures is demonstrated.

Figure 10 presents the final computed thickness distribution. It can be seen that the parison has been laterally displaced with respect to the extrusion axis. This has been found necessary to prevent a folding initiating during the handle blowing. This has been confirmed experimentally and a good compromise has to be found between this displacement and the associated low thickness values obtained at the bottom of the bottle, on opposite side.

The computing time is 1130s on a single processor of a Silicon Graphics R10000 origin 200 machine (412 time increments, maximum node number: 5000).

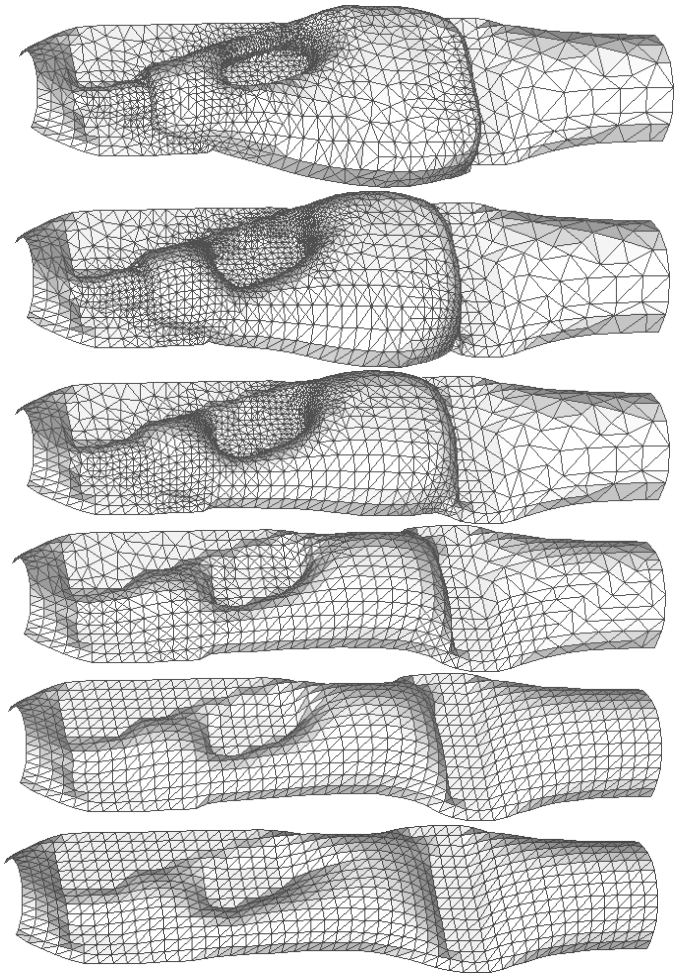

Figure 9. Simulation of the blow molding of a detergent bottle.

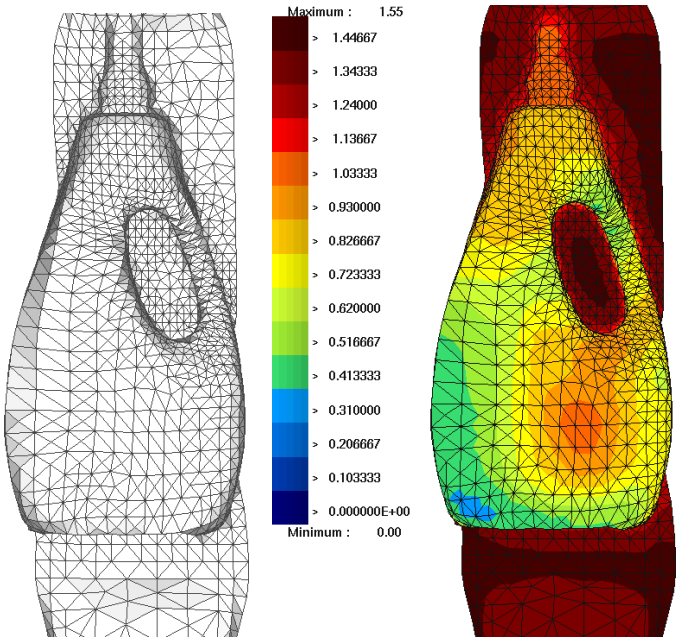

Figure 10. Final configuration of the simulated bottle. Deformed mesh and thickness profile (mm).

ACKNOWLEDGEMENT

This study has been supported by Elf-Atochem and Solvay companies. The experimental work has been carried out at Cerdato (Research Centre of Elf-Atochem, France).

REFERENCES

Bellet M., Massoni E., Chenot J.L., "*Numerical simulation of thin sheet forming processes by the finite element method*", Engng Comput., **7** (1990) 21-32

Bonet J., "*Error estimators and enrichment procedures for the finite element analysis of thin sheet large deformation processes*", Int. J. Num. Meth. Engng, **37** (1994) 1573-1591

Charrier J.M., Shrivastava S., Wu R., "*Free and constrained inflation of elastic membranes in relation to thermoforming*", J. Strain Analysis, **24** (1989) 55-74

Coupez T., "*Parallel adaptive remeshing in 3D moving mesh finite element numerical grid generation*", Computational Field Simulations, B.K.Soni et al. (eds.) (1996) 783-792.

Debbaut B., Hocq B., Marchal J.M., "*Numerical simulation of the blow molding process*", Proc. PPS'9 (1993) 329-330

De Lorenzi H.G., Nied H.F., "*Finite element simulation of thermoforming and blow molding*", Modelling of Polymer Processing, A.I.Isayev (ed.), Hanser, chap.5 (1991) 117-171

D'Oria F., Bourgin P., Coincenot L., "*Progress in numerical modelling of the thermoforming process*", Advances in Polymer Technology, **14** (1995) 291-301

Hartwig K., Michaeli W., "*Finite element simulation of the stretch blow molding process*", Proc. NUMIFORM'95, Balkema, Rotterdam (1995) 1029-1034

Kouba K., Bartos O., Vlachopoulos J., "*Computer simulation of thermoforming in complex shapes*", Polym. Eng. Sci., **32** (1992) 699-704

Laroche D., Diraddo R.W., Aubert R., "*Process modelling of complex blow-molded parts*", Plastics Engng, **52** (1996) 37

Rachik M., Roelandt J.M., Batoz J.-L., "*Simulation numérique du soufflage et du thermoformage des plastiques*", Revue Européenne des Eléments Finis, **3** (1994) 187-210

Rodriguez-Villa A., Agassant J.F., Bellet M., "*Finite element simulation of the extrusion blow-molding process*", Proc. NUMIFORM'95, Balkema, Rotterdam (1995) 1053-1058

Rodriguez-Villa A., "*Etude théorique et expérimentale de l'extrusion-soufflage de corps creux en polymère*", PhD thesis, Ecole des Mines de Paris (1997)

Santhanam N., Himasekhar K., Wang K.K., "*A design tool for blow-molding and thermoforming process*", Proc. NUMIFORM'95, Balkema, Rotterdam (1995) 1059-1063

Schmidt F.M., Agassant J.F., Bellet M., Desoutter L., "*Viscoelastic simulation of PET stretch/blow molding process*", Int. J. Non Newt. Fluid Mech., **64** (1996) 19-42

Shrivastava S., Tang J., "*Large deformation analysis of non-linear viscoelastic membranes with reference to thermoforming*", J. Strain Anal., **28** (1993) 31-51

Song W.N., Mirza F.A., Vlachopoulos J., "*Finite element analysis of inflation of an axisymmetric sheet of finite thickness*", J. Rheol., **35** (1991) 93-111

Vantal M.H., Monasse B., Bellet M., "*Numerical simulation of the thermoforming of multi-layer polymer sheets*", Proc. NUMIFORM'95, Balkema, Rotterdam (1995) 1089-1095

Verron E., "Contribution expérimentale et numérique aux procédés de moulage par soufflage et de thermoformage", PhD thesis, Ecole Centrale et Université de Nantes (1997)

Warby M.K., Whiteman J.R., "*Finite element model of viscoelastic membrane deformation*", Comp. Meth. Appl. Mech. Engng, **68** (1988) 33-54

Zhang K.F., Makinouchi A., Wang S., Nakagawa T., "*Process simulation of polymer blow molding by 3-D rigid visco-plastic FEM*", Proc. NUMIFORM'95, Balkema, Rotterdam (1995) 1097-1103